Synthesis and Pharmacological Characterization of Novel Analogues of the Nicotinic Acetylcholine Receptor Agonist (±)-UB-165

Christopher G. V. Sharples,[†] Gunter Karig,[‡] Graham L. Simpson,[‡] James A. Spencer,[‡] Emma Wright,[‡] Neil S. Millar,[§] Susan Wonnacott,*,[†] and Timothy Gallagher[‡]

Department of Biology and Biochemistry, University of Bath, Bath BA2 7AY, United Kingdom, School of Chemistry, University of Bristol, Bristol BS8 1HS, United Kingdom, and Department of Pharmacology, University College London, Gower Street, London WC1E 6BT, United Kingdom

(±)-UB-165 (**1**) is a potent neuronal nicotinic acetylcholine receptor (nAChR) ligand, which displays functional selectivity between nAChR subtypes. Using UB-165 as a lead structure, two classes of racemic ligands were synthesized and assessed in binding assays for three major nAChR subtypes (α4β2*, α3β4, and α7). The first class of compounds comprises the three pyridine isomers **4**−**6**, corresponding to the 3-, 2-, and 4-substituted pyridine isomers, respectively. Deschloro UB-165 (**4**) displayed a 2−3-fold decrease in affinity at α4β2* and α3β4 nAChR subtypes, as compared with (±)-UB-165, while at the α7 subtype a 31-fold increase in affinity was observed. At each of the nAChR subtypes, high affinity binding was dependent on the presence of a 3-substituted pyridine, and the other isomers, **5** and **6**, resulted in marked decreases in binding affinities. The second class of compounds is based on replacing the pyridyl unit of **1** with a diazine moiety, giving pyridazine (**7**), pyrimidine (**8**), and pyrazine (**9**), which retain the "3-pyridyl" substructure. Modest reductions in binding affinity were observed for all of the diazine ligands at all nAChR subtypes, with the exception of **7**, which retained potency comparable to that of **4** in binding to α7 nAChR. In functional assays at the α3β4 nAChR, all analogues **4**−**9** were less potent, as compared with **1**, and the rank order of functional potencies correlated with that of binding potencies. Computational studies indicate that the 3-substituted pyridine **4** and 2-substituted pyridine **5**, as well as the diazine analogues **7**−**9**, all conform to a distance-based pharmacophore model recently proposed for the α4β2* receptor. However, the nicotinic potencies of these ligands vary considerably and because **5** lacks appreciable nicotinic activity, it is clear that further refinements of this model are necessary in order to describe adequately the structural and electronic demands associated with this nAChR subtype. This rational series of compounds based on UB-165 presents a systematic approach to defining subtype specific pharmacophores.

Introduction

Neuronal nicotinic acetylcholine receptors (nAChRs) are pentameric ligand-gated cation channels, which are comprised of various combinations of α and β subunits (α2−10, β2−4).[1−3] Consequently, there is potential for huge diversity of nAChR subtypes and defining the subunit composition of native nAChRs is a considerable challenge. However, a few subtypes of nAChR predominate; notably, α4β2* and α7 subtypes are widespread in the vertebrate central nervous system (CNS).[4,5] The α4β2* nAChR binds nicotine with high affinity under equilibrium binding conditions and accounts for the majority of [³H]nicotine binding sites in rodent brain.[6] The α7 nAChR is considered to exist as a homopentamer[7,8] and is defined by high affinity binding of the specific ligands α-bungarotoxin (αBgt)[4] and methyllycaconitine (MLA).[9] In autonomic ganglia of the peripheral nervous system (and neuroblastoma cell lines derived from them), α3β4* nAChRs constitute the major

nAChR subtype;[10] these nAChRs bind [³H]epibatidine (but not [³H]nicotine) with relatively high affinity.[5,11]

Neuronal nAChRs are implicated in diverse CNS functions, including neuronal development, cognitive processing, and reward,[12] and have been linked to various clinical states including Alzheimer's and Parkinson's diseases, schizophrenia, and nociception.[13] Hence, neuronal nAChRs constitute a major target for drug discovery. The generation of subtype selective ligands to specifically target relevant nAChRs with a minimum of side effects, including those mediated through nAChRs expressed in the peripheral nervous system, is a goal. Understanding the molecular features of nicotinic drugs that define particular nAChR subtypes, and hence identification of nAChR subtype specific pharmacophores, would facilitate rational drug design.

Early nicotinic pharmacophore models were based on distances between pharmacophoric elements in the classical agonists, typically the distance between a basic nitrogen (which is protonated under physiological conditions) and a hydrogen bond-accepting moiety, typically a nitrogen (or carbonyl oxygen). N−N distances of 5.9 Å[14] or ranging from 4.4 to 5.0 Å[15] have been proposed, although the tolerance of the nAChR for the gross steric

---

* To whom correspondence should be addressed. Tel.: (44-1225)-826391. Fax: (44-1225)826779. E-mail: bsssw@bath.ac.uk.
† University of Bath.
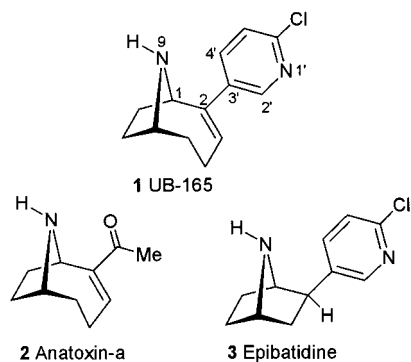‡ University of Bristol.
§ University College London.

Figure 1. Structures of UB-165 (**1**), anatoxin-a (**2**), and epibatidine (**3**).

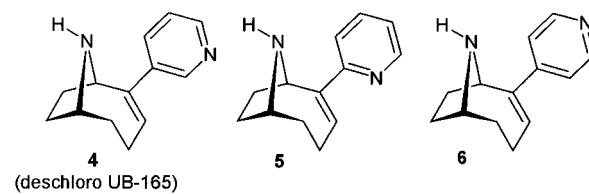**Figure 2.** Novel pyridine and diazine analogues.

bulk of the ligand was not considered. Indeed, more recent studies of high affinity binding to $\alpha 4\beta 2^*$ nAChR have indicated a more complex mode of action, which may implicate cationic π system interactions between ligand and receptor and vice versa.[16] This would be consistent with the presence of aromatic amino acids in the nAChR agonist binding site.[17]

The early pharmacophore models were largely based on knowledge of the interaction of nicotinic ligands with nAChRs in skeletal muscle and were developed before the extent of the heterogeneity of their neuronal counterparts was appreciated. Subtly different pharmacophores must exist not only for different nAChR subtypes but also for different states of a particular nAChR. A high affinity desensitized state is favored in radioligand binding assays whereas an activated state is measured in assays of nAChR function. Different molecular features may preferentially favor the stabilization of one state over the others. A complete subtype specific pharmacophore would aim to describe the molecular features that determine high affinity binding, receptor activation, and selectivity between nAChR subtypes. Indeed, the recent pharmacophore studies have focused on a specific nAChR ($\alpha 4\beta 2^*$): while the basis of the new models involves distance parameters, these are not based simply on the geometry (N–N distance) of the ligand.[16,18] The multidisciplinary combination of rational chemical synthesis of novel drugs and their subsequent evaluation in assays of biological activity enables us to address the key issues associated with developing and improving subtype specific neuronal pharmacophores.

UB-165 (**1**) is a rationally designed hybrid molecule consisting of a 9-azabicyclo[4.2.1]nonene ring coupled to a chloropyridine via C(3) of the pyridyl unit. The two major structural components—the azabicycle and the chloropyridine—are present in the molecular structures of the potent nicotinic agonists anatoxin-a (**2**) and epibatidine (**3**), respectively (Figure 1).

Compound **1** was conceived to probe the molecular basis of the enantioselectivity shown by nAChR.[19] The natural enantiomer (+)-anatoxin-a is 2 orders of magnitude more potent than (−)-anatoxin-a at muscle nAChR[20] and neuronal nAChR.[21] In contrast, the enantiomers of epibatidine are essentially equipotent.[22] UB-165 was found to preserve the enantioselectivity associated with anatoxin-a at rat brain nAChR.[19] This suggested that the observed enantioselectivity arises from the higher degree of dissymmetry associated with
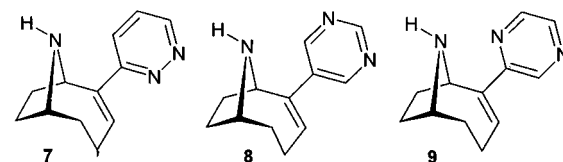
the 9-azabicyclo[4.2.1]nonene unit, in contrast to the smaller asymmmetric, but less dissymmetric, 7-azabicyclo[2.2.1]heptane ring present in epibatidine.[23,24] The high potency with which (±)-UB-165 binds to brain nAChR points toward this ligand as both a useful lead structure and a valuable probe for nAChRs, with potential as a tool to dissect the roles of individual nAChRs in physiological processes. In functional assays, (±)-UB-165 was found to be a potent but inefficacious partial agonist at $\alpha 4\beta 2^*$ nAChR in rat thalamic synaptosomes and at human $\alpha 4\beta 2$ nAChR expressed in *Xenopus* oocytes, and this property was exploited to implicate $\alpha 4\beta 2^*$ nAChR in the presynaptic modulation of [³H]dopamine release from isolated nerve terminals from rat striatum.[25]

UB-165 is a useful candidate for structure–activity studies as it is readily amenable to structural modification and possesses a semirigid molecular skeleton, which restricts the number of stable conformations and hence eases mapping of a pharmacophore. Modifiying UB-165 may lead to the generation of novel ligands, which are able to further discriminate between nAChR subtypes. The chloro moiety of UB-165 does not appear to contribute significantly toward biological potency (see below), and for the purposes of synthetic accessibility, this component has not been retained. Our initial investigations into structural variants of UB-165 have focused on the generation of two groups of molecules in which the heteroaryl (pyridyl) component of UB-165 has been varied (Figure 2).

Class 1 comprises the three pyridyl isomers: **4** (the deschloro analogue of UB-165) and the 2-pyrido and 4-pyrido analogues **5** and **6**, respectively. Class 2 explores further modification of the heteroaryl component by incorporation of an additional nitrogen (i.e., diazines rather than pyridines), and we have synthesized the pyridazine, pyrimidine, and pyrazine analogues **7**–**9**, respectively. It should be noted that while there are other diazine isomers possible, we have restricted the isomers prepared to those that retain the "3-pyridyl" substructure associated with **1** and **4**. The reasons for this restriction are discussed in more detail below. Both classes of compounds have been examined for binding affinity at the $\alpha 4\beta 2^*$ and $\alpha 7$ nAChRs expressed in rat brain and at the rat $\alpha 3\beta 4$ nAChR expressed in a stably transfected cell line. In addition,

Scheme 1[a]

For ligand classification and
yields, see Fig.2 and below
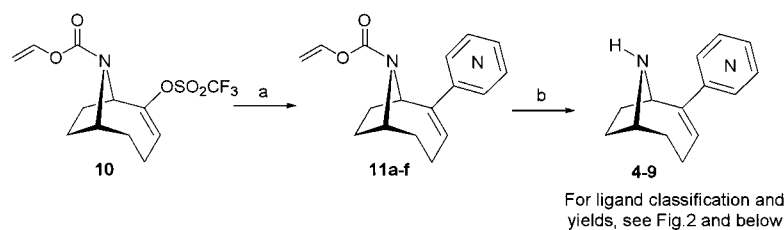
ArZnX	Class 1[a]	ArZnX	Class 2[a]
	 4 (70 %)		 **7** (87 %)
	 5 (84 %)		 **8** (77 %)
 (see text)	 **6** (64 %)[b]		 **9** (80 %)

[a] Reagents: (a) ArZnX, Pd(PPh₃)₄, THF. (b) HCl, H₂O. (a) The overall yield for step a (Pd(0) cross coupling) and step b (N deprotection) in Scheme 1, respectively. Ligands **4−9** were isolated as the corresponding hydrochloride salts. (b) This represents the overall yield for the formation of **6** for Pd-mediated coupling,[26] reduction of the intermediate 3-bromo residue, and *N*-Voc cleavage.

functional potency at the $\alpha 3\beta 4$ nAChR was assessed using a calcium fluorescence assay.

Results and Discussion

Chemistry. ($\pm$)-UB-165 (**1**) has provided an initial lead, and we now describe the synthesis of two classes of analogues based on (i) positional isomers of the pyridyl moiety (class 1) and (ii) selected diazine variants (class 2). The synthetic strategy employed for both classes of ligands is shown in Scheme 1 and is based on the route developed originally for **1**.

In this process, the key step is a Negishi Pd(0)-mediated cross-coupling of vinyl triflate **10** with the appropriate heteroaryl zinc halide (ArZnX) using Pd-(PPh₃)₄ as the catalyst to provide coupled adducts **11a−f**. Following isolation and purification, the N-vinyloxy-carbonyl protecting group of **11** underwent essentially quantitative acidic cleavage, and final products **4−9** were isolated and screened as the corresponding hydrochloride salts. This approach provided all of the analogues described in this paper, with the exception of the 4-pyridyl derivative **6**. In this case, we were unsuccessful in generating the requisite 4-pyridylzinc halide needed, and indeed vinyl triflate **10** also failed to couple to a variety of other 4-pyridyl organometallic reagents based on Suzuki and Stille conditions. As a result, a procedure has been developed, which represents a new method for the synthesis of 4-substituted pyridines, including the 4-pyridyl analogue **6**. This is based on the

use of a (3-bromo-4-pyridyl)zinc halide (see Scheme 1).[26] Once the Negishi coupling step was complete, the bromo directing group was removed by selective reduction to provide **11c**, which then underwent cleavage of the N-vinyloxycarbonyl moiety to give **6** (Scheme 1).

Binding Assays. Compound **1** and the two classes of analogues based on UB-165 were tested for their binding affinities at the major nAChR subtypes present in the CNS and peripheral nervous system. These comprised the rat brain $\alpha 4\beta 2$* and $\alpha 7$ nAChRs, which were labeled by [³H]nicotine and [³H]MLA, respectively, and the rat $\alpha 3\beta 4$ nAChR expressed in a stably trans-fected cell line[27] and labeled by [³H]epibatidine. The binding affinities of ($\pm$)-UB-165 (**1**) at $\alpha 4\beta 2$* and $\alpha 3\beta 4$ nAChR (K_i = 0.27 and 6.5 nM, respectively) were intermediate between those of ($\pm$)-anatoxin-a (**2**) and ($\pm$)-epibatidine (**3**), with the potency order **3** > **1** > **2**. At the $\alpha 7$ nAChR, the potency order was **3** > **2** > **1**, with a K_i value of 2760 nM for **1** (Table 1).

To facilitate future chemical modification of the heteroaryl component, the deschloro analogue **4** of **1** was synthesized and evaluated. This modification resulted in a 2−3-fold decrease in binding affinity of **4** at the $\alpha 4\beta 2$* and $\alpha 3\beta 4$ nAChRs, as compared with **1**. Thus, the chlorine atom is not crucial for nicotinic activity and its presence has little influence on the binding potency of **1** at these nAChR subtypes. Similarly, the analogous modification of epibatidine did not change binding affinity at rat brain $\alpha 4\beta 2$* nAChR with respect to the

Table 1. Binding Affinities Values of Compounds at nAChR Subtypes

	nAChR subtype		
	K_i (nM)^a (affinity ratio)^b		
compd	α4β2*	α3β4	α7
(±)-UB-165 (**1**)	0.27 ± 0.05 (1)	6.5 ± 2.3 (24.1)	2760 ± 473 (10 222)
(±)-anatoxin-a (**2**)	1.25 ± 0.2 (1)	25.4 ± 1.9 (20.3)	1140 ± 124 (1472)
epibatidine (**3**)	0.021 ± 0.005 (1)	0.077 ± 0.008 (3.7)	101 ± 16 (4810)
4	0.43 ± 0.03 (1)	22.5 ± 5.5 (52)	89 ± 35 (207)
5	1540 ± 280 (1)	10 500 ± 1650 (6.8)	47 500 ± 11 050 (31)
6	10 950 ± 1225 (1)	22 000 ± 4770 (2)	>50 000 (−)
7	2.6 ± 0.2 (1)	306 ± 51 (20)	68.4 ± 16.2 (118)
8	2.45 ± 0.37 (1)	236 ± 30 (96)	1706 ± 223 (696)
9	58 ± 13 (1)	2846 ± 484 (49)	5773 ± 484 (100)

^{a} Results are the mean of at least three independent determinations ± SEM. ^{b} Affinity ratio is the potency relative to that at the α4β2* nAChR.

parent molecule.[22] Moreover, chlorination of nicotine also had a minimal influence on binding affinity at rat brain α4β2* nAChR.[23,28] However, at the α7 nAChR, a 31-fold increase in affinity for **4**, as compared with **1**, was observed, suggesting that at this nAChR subtype a small advantage arises from the loss of the halogen.

Deschloro UB-165 (**4**) was compared with the two other pyridyl isomers, comprising our first class of analogues, to explore the effect of translocation of the pyridyl nitrogen, which is proposed to act as a hydrogen bond acceptor in models of the nicotinic pharmacophore.[14–16,29] As compared to the 3-substituted pyridines (represented by UB-165 and the deschloro analogue **4**), the 2-pyrido analogue **5** and the 4-pyrido analogue **6** represent structures in which the distance between the cationic nitrogen and the pyridyl nitrogen has been respectively decreased and increased. For both **5** and **6**, substantially diminished binding affinities at all nAChR subtypes examined were observed and this points toward the importance of a nitrogen atom in the 3′ position (as in **4**). As compared with **4**, the 2-pyridyl variant **5** was 3581-fold less potent at the α4β2* nAChR with smaller decreases in potency of 467- and 534-fold at the α3β4 and α7 nAChR, respectively. The 4-pyridyl derivative **6** resulted in even greater reductions in affinity at each of these nAChR subtypes, and as for **5**, the greatest decrease was at the α4β2* nAChR with a 25 419-fold loss of potency. Smaller decreases of 978 and >562-fold were observed for **6** at the α3β4 and α7 nAChRs, respectively (Table 1).

The second class of compounds incorporates a diazine moiety, but the design had certain constraints imposed. Given that a 3-pyridyl unit seems to be a requisite for high affinity binding, we have restricted the diazine class to those that retain this feature. We have synthesized and evaluated three isomeric diazine analogues: pyridazine **7**, pyrimidine **8**, and pyrazine **9**. The presence of an additional nitrogen atom produces a more π-electron deficient aromatic ring, and this exerts a significant effect on the pK_a of the nitrogen atom representing the hydrogen bond acceptor associated with the ligand–receptor interaction.[30] Pyridine (pK_a 5.22) is significantly more basic than pyridazine (pK_a 2.33), pyrimidine (pK_a 1.31), and pyrazine (pK_a 0.65), and the value of this type of structural variation in medicinal chemistry has been recognized as a useful tool.[31] The pyrimidine analogue **8** was slightly less potent than **4** at all nAChR subtypes, with respective decreases in binding affinity of 6-, 10.5-, and 19.2-fold

at α4β2*, α3β4, and α7 nAChR. At the α4β2* subtype, a similar 5-fold decrease in binding potency was reported for a pyrimidinyl derivative of epibatidine.[32] Pyrazine **9** resulted in greater decreases in potency than **7** or **8** at all nAChR subtypes relative to **4**, with decreases in binding affinity of 135-, 32-, and 257-fold at α4β2*, α3β4, and α7 nAChR, respectively (Table 1). Pyridazine **7**, like pyrimidine **8**, was slightly less potent at α4β2* and α3β4 nAChRs as compared with **4**, with respective decreases in binding potency of 6- and 13.6-fold. These results indicate that the presence of a diazine will generally decrease binding affinity with the greatest impact being exerted by an addition of a nitrogen at the 6′ position, as in pyrazine **9**. However, **7** differed from **8** and **9** in retaining activity at the α7 nAChR: it was the most potent of all of the analogues examined in this study at the α7 nAChR (Table 1), binding with a potency comparable to that of **4**.

Compounds **1**−**9** had the following rank orders of potency for binding to each nAChR subtype: α4β2* **3** > **1** > **4** > **2** > **7** = **8** > **9** ≫ **5** ≫ **6**; α3β4 **3** > **1** > **4** = **2** > **8** > **7** > **9** ≫ **5** ≫ **6**; and α7 **7**, **4** > **3** > **2** > **8** > **1** > **9** ≫ **5** ≫ **6**. The rank order profiles of compound potencies at α4β2* and α3β4 nAChRs are very similar whereas the profile at α7 nAChR is more divergent. This implies that α7 nAChR possesses a pharmacophore that is distinct from that of α4β2* and α3β4 nAChRs.

nAChR Subtype Selectivity. The binding affinities of compounds **1**−**9** were compared to examine subtype selective interactions (Table 1). (±)-UB-165 (**1**) was more selective for α4β2* nAChR over α3β4 and α7 nAChR than (±)-anatoxin-a (**2**) and (±)-epibatidine (**3**). Relative to α4β2*, (±)-UB-165 had a 24- and 10 222-fold difference in potency at α3β4 and α7 nAChR, respectively, as compared to (±)-anatoxin-a, which had 20- and 1472-fold differences, and (±)-epibatidine, which had 3.7- and 4810-fold differences, respectively. This selectivity for the α4β2* nAChR vs the α7 nAChR is decreased in **4** to 207- vs 10 222-fold. However, **4** exhibits increased selectivity with respect to α3β4 nAChR (52- vs 24-fold). nAChR subtype selectivity was greatly decreased in the pyridyl isomers **5** and **6**. Pyrimidine **8** was more selective for the α4β2* nAChR over α7 and α3β4 nAChR than **4** (respective potency differences of 696- and 96-fold). In contrast, pyridazine **7** and pyrazine **9** had a poorer selectivity profile for the α4β2* nAChR: **7** had 20- and 118-fold differences in potency, and **9** had 49- and 100-fold differences in potency at α7 and α3β4 nAChRs, respectively.

Table 2. Activation Potencies of Compounds at the $\alpha3\beta4$ NAChR

compd	EC_{50} $(\mu M)^a$	$(EC_{50}/K_i)^b$
($\pm$)-UB-165 (**1**)	0.31 ± 0.07	48
($\pm$)-anatoxin-a (**2**)	2.29 ± 0.69	90
($\pm$)-epibatidine (**3**)	0.014 ± 0.002	182
4	1.59 ± 0.31	71
5	>100	
6	>100	
7	4.19 ± 0.99	14
8	3.89 ± 0.20	16
9	>100	

^{a} EC_{50} is the concentration required to achieve a half-maximal activation. Results are the mean of at least three independent determinations $\pm$ SEM. ^{b} K_i values are taken from Table 2.

Functional Studies—Activation of $\alpha3\beta4$ nAChR. ($\pm$)-UB-165 (**1**) and the analogues described in this study were also tested for their functional potency at the $\alpha3\beta4$ nAChR, stably expressed by the L$\alpha3\beta4$ cell line.[27] This assay was performed in order to confirm that occupation of the agonist binding site, as shown in competition radioligand binding assays, leads to receptor activation. The functional assay monitored increases in the fluorescence of a calcium sensitive dye, fluo-3, upon agonist stimulation. ($\pm$)-UB-165 (**1**) evoked increases in intracellular calcium with an EC_{50} value of 0.31 μM, intermediate between that of ($\pm$)-epibatidine (**3**) and that of ($\pm$)-anatoxin-a (**2**), which gave EC_{50} values of 0.014 and 2.29 μM, respectively (Table 2, Figure 3). Compound **4** had a slightly reduced EC_{50} value of 1.59 μM while **5** and **6** were essentially inactive over the concentration range examined, with EC_{50} values >100 μM. Given the small amounts of compound available, it was not practical to extend the dose–response curves to determine full functional dose–response relationships. However, these results do indicate a critical role for the positioning of the pyridyl nitrogen and support a role for internitrogen distances in determining functional potency. Similar results were also observed by Spang and colleagues on $\alpha3\beta4$ nAChR expressed in *Xenopus* oocytes: the (+) and (−) enantiomers of the deschloro epibatidine analogue 2PABH (cf. **5** in the present study) were 406- and 2952-fold, respectively, less potent than deschloro epibatidine.[33]

The pyridazinyl and pyrimidinyl derivatives **7** and **8** had only slightly reduced potencies when compared to **4** (respective EC_{50} values of 4.19 and 3.89 μM), while pyrazine **9** had a greatly reduced potency (EC_{50} value > 100 μM). EC_{50} values are about 2 orders of magnitude greater than corresponding K_i values for each compound, as greater concentrations of agonist are required to stabilize the activated state of the nAChR (represented by the EC_{50} value) than the high affinity desensitized state, which is represented by the K_i value.[34] The ratio of EC_{50}/K_i for **7** and **8** (16- and 14-fold, respectively) was decreased as compared to **4** (71-fold). Thus, the presence of a second nitrogen (diazine vs pyridine) may decrease the difference in affinities of ligand interaction with the activated and desensitized receptor states, which are measured in functional and binding assays, respectively.

Computational Studies. As alluded to earlier, a compelling role for structure–activity relationships is to define and develop new pharmacophore models with specificity for individual receptor subtypes. While this
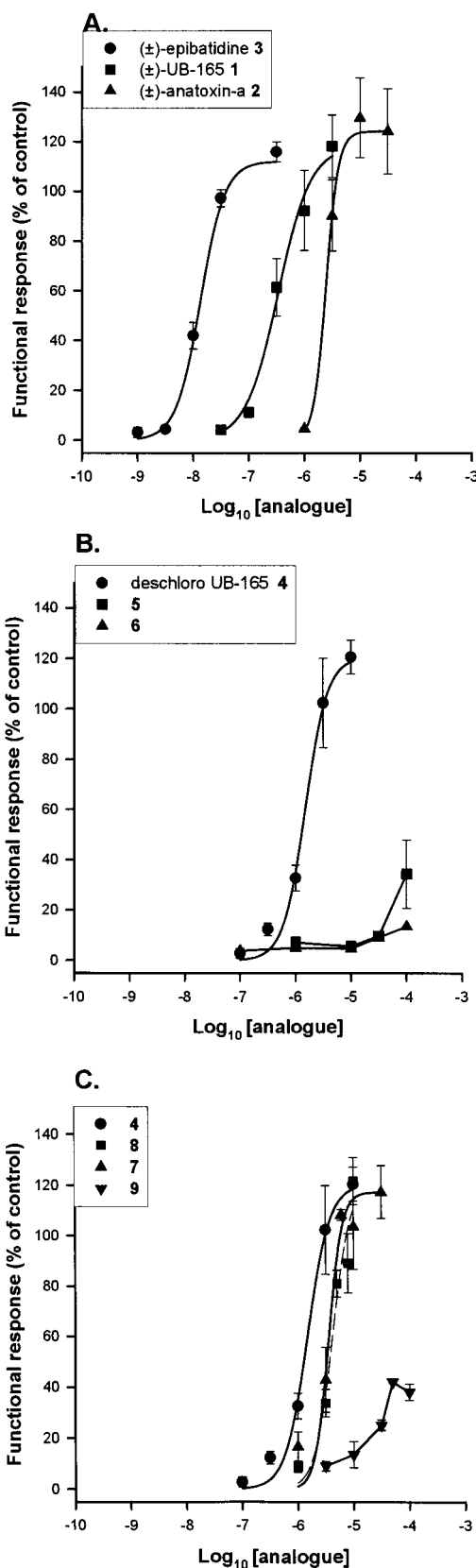
Figure 3. Dose–response relationships for agonist-induced increases in intracellular calcium, as measured by fluo-3 fluorescence, evoked by (A) ($\pm$)-UB-165 (**1**), ($\pm$)-anatoxin-a (**2**), and ($\pm$)-epibatidine (**3**); (B) **4**–**6**; (C) **4** and **7**–**9** at the $\alpha3\beta4$ nAChR expressed in L$\alpha3\beta4$ cells. Functional responses are expressed as the percentage of a maximally efficacious concentration of (−)-nicotine (100 μM). Vertical bars indicate the SEM from at least three independent determinations.

goal is still some way off, it is instructive to compare the molecules discussed in this paper against current pharmacophore models. Internitrogen (N−N) distances have been linked to nicotinic activity, with a value of 4.8 ± 0.3 Å derived for the classic Beers−Reich (and later Sheridan) models.[14,15] Glennon and co-workers have shown that for epibatidine (one of the most potent agonists known) the N−N distance (5.51 Å) exceeds this value.[23,35] However, the N−N distance of **3** (and indeed most other ligands) is dependent on the conformation selected for measurement, and others have recognized that alternative low energy conformations of **3** with N−N distances ranging from 4.7 to 5.5 Å may nevertheless be significant in terms of bioactivity.[36] Furthermore, Danish workers have suggested that the N−N distance in isolation is not the essential (or unique) pharmacophore component.[18,36] Rather, a refined series of distance relationships have been proposed, which are associated with the putative ligand−receptor complex. This has led to an improved pharmacophore model for the $\alpha 4 \beta 2^*$ nAChR.[18] This model consists of (i) a point corresponding to a protonated nitrogen atom, (ii) a point corresponding to an electronegative atom capable of forming a hydrogen bond, and (iii) the center of a heteroaromatic ring or a C=O bond. These elements were related by the following parameters: an (a−b) distance of 7.3−8.0 Å, an (a−c) distance of 6.5−7.4 Å, and an angle of 30.4−35.8° between the two distance vectors (Δbac). Given the ongoing debate, we have examined the structural properties of ligands **4**−**6** in terms of these alternative pharmacophore concepts, and the key structural parameters are summarized in Table 3.

Figure 4a,b shows, respectively, the conformational profiles (based on the C(1)−C(2)−C(3)−C(2′) torsion angle—see also footnote b, Table 3) of the pyridine isomers **4** (deschloro UB-165, the 3-substituted isomer) and **5** (the 2-substituted isomer); the N−N distances associated with the low energy conformer populations are indicated.

In the case of **4**, the N−N distances range from 4.84 to 5.81 Å (if conformers up to 5 kJ mol^{-1} above the local minima are also recognized). This certainly encompasses the Beers−Reich distance (4.8 ± 0.3 Å) but at the higher end of the range, and conformations with larger N−N distances are also easily accessible.

For the 2-substituted pyridine analogue **5**, the N−N distances are generally shorter, ranging from 3.8 to 4.8 Å, and the variation in conformational minima (as compared to **4**) is more dramatic, which presumably reflects destablizing interactions associated with the pyridine nitrogen lone pair and the azabicycle. For the 4-substituted pyridine **6**, the N−N distance (6.1 Å) is essentially independent of torsion angle changes associated with rotation of the heteroaryl unit. It is interesting to recall that unlike **4**, both **5** and **6** are weak nicotinic ligands.

The (a−b) distance and the bac angle (Δbac) associated with the Tønder pharmacophore for the $\alpha 4 \beta 2^*$ nAChR have been shown to correlate well to nicotinic binding potency.[18] We have calculated the (a−b) and Δbac parameters for compounds **4**−**6** (Table 3).

For the most potent analogue, **4**, the (a−b) distance and Δbac values at the global minimum (point 2 in

Table 3. Pharmacophore Parameters for Compounds **4**−**6**

	energy^a (kJ)	torsion^b (deg)	N−N distance^c (Å)	(a−b)^d (Å)	Δbac^d (deg)
		Compound **4**^{a}			
point 1	+5	29.5	5.1	7.0	36.1
point 2	global minimum	55	5.1	7.35	35.4
point 3	+1.8	122.5	5.5	9.5	26.8
point 4	+6.8	150	5.7	10.3	20.0
point 5	+8.2	215	5.9	10.8	9.2
point 6	+3.2	238	5.9	10.6	15.1
point 7	+1.8	308	5.5	8.6	31.6
point 8	+6.8	332	5.4	7.8	34.2
		Compound **5**^{a}			
point 1	+6	51	3.8	3.2	25.6
point 2	+4.6	138	4.4	7.4	34.8
point 3	+2.7	229	4.8	8.7	30.8
point 4	global minimum	311	4.3	6.0	36.8
point 5	+5	338	4.1	4.6	35.2
		Compound **6**^{e}			
			6.0	10.1	25.4

^{a} Conformational and distance properties measured at points shown in see Figure 4a for deschloro UB-165 (**4**) and Figure 4b for analogue **5**, including at values associated with conformations 5 kJ higher in energy than the local minima. Energy values shown are relative to the global minimum position. ^{b} Torsion angle is defined by C(1)−C(2)−C(3′)−C(2′) as illustrated in structure **1**. In the case of compound **5** (incorporating a 2-substituted pyridine), the equivalent dihedral corresponds to C(1)−C(2)−C(2′)−N(1′). ^{c} Beer−Reich internitrogen (N−N) distance. ^{d} (a−b) and Δbac parameters corresponding to the $\alpha 4 \beta 2^*$ pharmacophore model.[18] Point a was derived as described in the literature using the N(9) lone pair, which is formally (given that N(9) is assumed to be protonated when bound to the receptor) anti to the larger four carbon ring of the 9-azabicyclo[4.2.1]non-2-ene moiety. ^{e} Compound **6** clearly has a wide range of conformational states available and displays a profile that is very similar to that shown in Figure 4a for compound **4**. However, the symmetry of the 1,4-disubstituted pyridine unit of **6** means that the pharmacophore parameters (N−N distance, as well as (a−b) and Δbac) remain constant and independent of rotation about the key torsion angle, which is now C(1)−C(2)−C(4′)−C(3′).

Figure 4a) are 7.35 Å and 35.4°, respectively: these values lie within the optimal range for the $\alpha 4 \beta 2^*$ nAChR pharmacophore (see above).[18] Distance and angle values for other low energy conformations do not, however, fall within the accepted range.

The (a−b) distances determined for **5** range from 3.2 to 8.7 Å, with Δbac values of 25.6−36.8°. The optimal (a−b) distance (which was shown to be the most reliable parameter for correlating nicotinic potency)[18] and Δbac value can be achieved by compound **5** (e.g., at point 2 in Figure 4b). However, this ligand shows markedly reduced affinity (as compared to **4**) for the $\alpha 4 \beta 2^*$ nAChR. This raises two issues. First, the conformation of **5**, which meets the $\alpha 4 \beta 2^*$ parameters, lies well above (+4.6 kJ) the global minima. Although this does not of itself preclude this being of bioactive significance, conformation populations associated with **5** will nevertheless be heavily biased away from this "preferred" arrangement. Interestingly, this is in contrast to **4** where the $\alpha 4 \beta 2^*$ pharmacophore parameters are met by, inter alia, a conformation located at the global minimium. Second, biological activity is influenced by binding of the ligand per se and not just by individual, albeit important, components; with one exception,[37] current pharmacophore models do not recognize interactions associated with other structural components of the ligand (see below).

Conformation of compound **4** at Point 2 in Figure 4a

Conformation of compound **5** at Point 2 in Figure 4b

Figure 5. Space-filling representations of compounds **4** and **5** using conformations with (a−b) and Δbac parameters fitting the proposed α4β2* nAChR pharmacophore.[18]
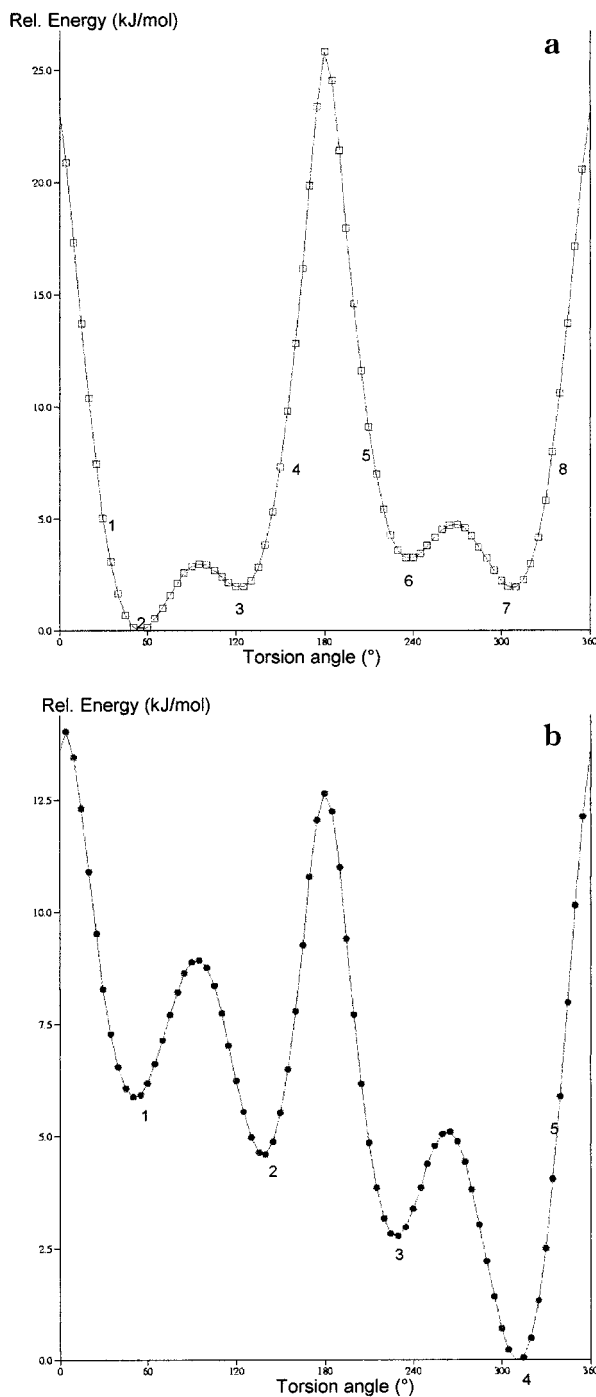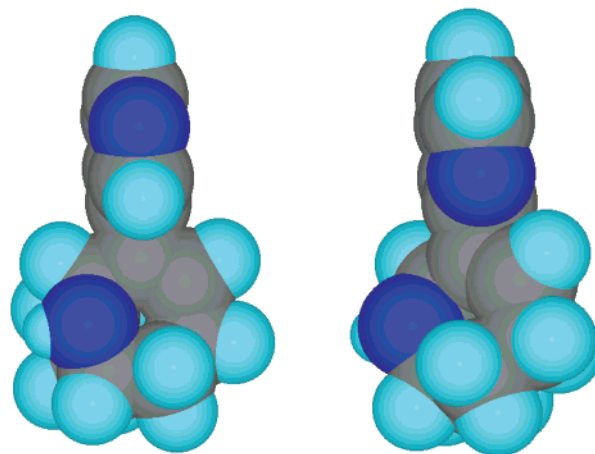

Figure 4. Conformational profiles of compounds **4** (a) and **5** (b).

In the case of compound **6**, symmetry dictates that the N−N distance (measured at 6.00 Å) and (a−b) (10.1 Å) and Δbac (25.4°) values are independent of the C(1)−C(2)−C(3′)−C(2′) torsion angle, but in this case, none of these parameters fall within the range of optimal values required and **6** interacts with α4β2* nAChR with diminished potency relative to **4** and **5**.

Like **4**, the class 2 compounds **7**−**9** also conform to the basic pharmacophoric elements for the α4β2* nAChR because a "3′-pyridyl" moiety is present in each of these ligands. (The presence of the pyrimidine component within **8** offers this ligand an entropic (statistical) advantage over **7** and **9**, but the significance, if any, of this remains to be demonstrated.) However, the nicotinic

potencies of this group of ligands are markedly different to that of **4**, and the relationship between diazine structure and hydrogen bond acceptor properties[30,31] has already been highlighted (see also the note added in proof). Clearly, as the structure−activity relationship of these and related compounds is developed further, these data will present an opportunity to refine the pharmacophore for the α4β2* nAChR, as well as develop pharmacophore models appropriate to other nicotinic receptor subtypes.

Additional factors must also be considered in developing pharmacophore models, and these include other structural parameters, such as the bulk and the electronic/hydrophobic properties of the azabicyclo[4.2.1]-nonene scaffold associated with the ligands reported in this paper. The interactions associated with this aspect of ligand structure, while not considered explicitly by either of the pharmacophore models discussed above (however, see ref 37), must nonetheless be accommodated within the relevant receptor−ligand complex. Both **4** and **5** can meet the (a−b) and Δbac demands associated with the α4β2* nAChR pharmacophore[18] but using quite different torsion angles and therefore different conformations. These conformational changes result in a "relocation" of the hydrophobic bulk of the 9-azabicyclo[4.2.1]non-2-ene moiety within the active site (relative to the two nitrogen-based pharmacophore sites) for **4** vs **5**, which is illustrated in Figure 5.

In the case of compound **5**, which although able to meet certain pharmacophore parameters still lacks appreciable nicotinic activity, the need to accommodate the sterically demanding molecular scaffold of the bicyclic moiety within the binding site may, in turn, inhibit the ligand−receptor interaction. Further refinements of pharmacophore models must consider those parts of the ligand that, while not directly involved in the primary binding interaction, may nevertheless exert a negative (or indeed positive) influence on the accessibility and acceptability of the ligand to the receptor binding site. One way forward will be to probe the ability of individual receptors to accommodate ligands carrying the same array of primary binding components

but held within a larger bicyclic framework, and this is currently under investigation.

Conclusions

Chemical modification of **1** has produced a series of analogues, which have been utilized to probe biological activity at three major neuronal nAChR subtypes. High affinity binding of **1** is critically dependent on the presence of the hydrogen bond-accepting pyridyl nitrogen in the 3′ position, as in **1** and **4**. Repositioning the pyridyl nitrogen to the 2′ or 4′ positions (as in **5** and **6**, respectively) leads to either a decrease or an increase in the distance from the cationic nitrogen present on the 9-azabicyclo[4.2.0]nonene ring, resulting in substantial decreases in binding affinity with respect to **4**. Replacing the pyridyl unit with a diazine moiety that retains the "3-substituted pyridine" unit leads to diminished binding potency, as compared with **4**. This was true for all nAChR subtypes with the exception of the pyridazine analogue **7**, which retained potency at α7 nAChR. For activation of α3β4 nAChR, functional assays demonstrated a similar potency relationship as for binding to this nAChR subtype with the rank order **3** > **1** > **4** ≥ **2** > **7** = **8** (**5**, **6**, and **9** were essentially inactive at the concentrations tested). Computational studies involving low energy conformers of compounds **4**−**6** show agreement with an α4β2* pharmacophore model in the case of **4** and **5**, but **6** was unable to meet the pharmacophore parameters. Because **5** lacks appreciable nicotinic activity, this indicates that further refinements of pharmacophore models are necessary. In summary, **1** has provided a useful framework for the generation of a series of analogues to informatively explore the molecular determinants of nAChR drug interaction.

Experimental Section

Chemistry. General Comments. Proton and carbon assignments are based on a combination of ^1H−^1H and ^1H−^{13}C COSY and DEPT spectra. For **10** and **11a**−**f**, which incorporate an N-vinyloxycarbonyl (Voc) moiety, carbamate resonance resulted in broadened ^1H and ^{13}C spectra, which resulted in significant, though not universal, doubling of lines. Where doubling of signals was apparent, this has been indicated.

9-Vinyloxycarbonyl-9-azabicyclo[4.2.1]nonan-2-one. To a solution of 9-methyl-9-azabicyclo[4.2.1]nonan-2-one in dry dichloromethane (95 mL) was added anhydrous potassium carbonate (4.13 g, 29.67 mmol), and the solution was stirred at room temperature for 1 h. The mixture was cooled to 0 °C, vinyl chloroformate (1.34 mL, 14.84 mmol) was added slowly, and the solution was stirred at room temperature for 24 h, after which time, further vinyl chloroformate (1.34 mL, 14.84 mmol) was added and stirring was continued for another 24 h. Silica gel was added, and the solvent was removed in vacuo. The residue was purified by flash chromatography (3:1 hexane: ethyl acetate) to give 9-vinyloxycarbonyl-9-azabicyclo[4.2.1]-nonan-2-one (1.95 g, 94%) as a colorless oil. IR (film) ν (cm^{-1}): 1715, 1648. ^1H NMR (300 MHz, CDCl$_3$): 7.26 (0.4 H, d d, $J =$ 14.0, 6.3 Hz, Voc), 7.18 (0.6 H, d d, $J =$ 14.0, 6.3 Hz, Voc), 4.88 (0.4 H, d d, $J =$ 14.0, 1.6 Hz, Voc), 4.77 (0.6 H, d d, $J =$ 14.0, 1.6 Hz, Voc), 4.65−4.61 (1 H, m), 4.51 (0.4 H, d d, $J =$ 6.2, 1.7 Hz, Voc), 4.48−4.42 (1.6 H, m), 2.68−2.56 (1 H, m), 2.49−1.58 (9 H, m). ^{13}C NMR (75 MHz, CDCl$_3$): 214.3 (C), 151.3 (C), 142.1 (CH), 96.0 (CH$_2$), 64.8 (CH), 56.9 (CH), 41.7 (CH$_2$), 33.5 (CH$_2$), 33.0 (CH$_2$), 26.6 (CH$_2$), 19.2 (CH$_2$). MS (60 eV): m/z 209 (M$^+$, 9%), 83 (100). HRMS: calcd for C$_{11}$H$_{15}$NO$_3$, 341.0545; found, 341.0552.

2-[(Trifluoromethyl)sulfonyloxy]-9-vinyloxycarbonyl-9-azabicyclo[4.2.1]non-2-ene (10). To a solution of 9-vinyl-oxycarbonyl-9-azabicyclo[4.2.1]non-2-one (1.6 g, 7.6 mmol) in dry tetrahydrofuran (THF, 60 mL) cooled to −78 °C was added KHMDS (0.5 M in toluene, 16.9 mL, 8.42 mmol), and the solution was stirred at −78 °C for 1.75 h. 2-[N,N-Bis(trifluo-romethylsulfonyl)amino]-5-chloropyridine (2.53 g, 7.6 mmol) in dry THF (30 mL) was then added via cannula. The reaction mixture was stirred at −78 °C for 4 h and then allowed to warm to room temperature. The solvents were removed in vacuo, and the crude material was purified by flash chroma-tography (eluting with 4:1 hexane:ethyl acetate) to give vinyl triflate **10** (1.70 g, 65%) as a colorless oil. IR (film) ν (cm^{-1}): 1717, 1238, 1067. ^1H NMR (400 MHz, CDCl$_3$): 7.24−7.15 (1 H, m, Voc), 5.80 (1 H, m, 3-H), 4.88−4.47 (4 H, m, Voc and 1-H, 6-H), 2.31−1.69 (8 H, m). ^{13}C NMR (75.5 MHz, CDCl$_3$): 153.3 (C), 142.2/141.8 (CH), 121.3/121.0 (CH), 116.4 (C), 96.0/ 95.8 (CH$_2$), 58.7/58.5 (CH), 55.4/55.3 (CH), 32.0/30.7 (CH$_2$), 30.7/29.8 (CH$_2$), 28.8/27.8 (CH$_2$), 19.8 (CH$_2$) (CF$_3$ was not observed). MS (70 eV): m/z 341 (M$^+$, 8%), 332 (9), 298 (90), 84 (100). HRMS: calcd for C$_{12}$H$_{14}$F$_3$NO$_5$S, 341.0545; found, 341.0552.

The following procedures were used to prepare all compounds shown in Scheme 1 (with the exception of the 4-pyridyl variant **6**) and are illustrated by the conversion of vinyl triflate **10** via **11b** to the 2-pyridyl derivative **5** as a specific example. Characterization data for individual compounds are then listed below, and full details for the preparation of **6** are provided here.

General Procedure 1. Pd(0)-mediated cross-coupling of vinyl triflate **10** to ArZnX was performed to give adducts **11a**−**f**.

2-(2-Pyridinyl)-9-vinyloxycarbonyl-9-azabicyclo[4.2.1]-non-2-ene (11b). A solution of 2-bromopyridine (136 mg, 0.855 mmol) in dry THF (7 mL) was cooled to −78 °C under a nitrogen atmosphere and ^{n}BuLi (1.6 M in hexanes, 0.53 mL, 0.86 mmol) was added dropwise. The solution was then stirred at −78 °C for 20 min. Anhydrous zinc chloride (117 mg, 0.855 mmol) in dry THF (3 mL) was added, and the solution was allowed to warm to room temperature. Triflate **10** (108 mg, 0.317 mmol) in dry THF (7 mL) was then added via a cannula followed by a solution of Pd(PPh$_3$)$_4$ (11.6 mg, 0.0095 mmol) in dry THF (3 mL) also via a cannula. The resulting solution was heated at reflux for 1 h and then allowed to cool and quenched with saturated aqueous ammonium chloride solution (30 mL). The organic layer was separated, and the aqueous layer was extracted with diethyl ether (3 × 20 mL). The combined organic phases were dried (Na$_2$SO$_4$), the solvent was removed in vacuo, and the residue was purified by flash chromatography (1:3 ethyl acetate:hexane) to give the title compound **11b** (72 mg, 84%) as a pale yellow oil. IR (film) ν (cm^{-1}): 1713, 1420, 1147. ^1H NMR (300 MHz, CDCl$_3$): 8.57 (1 H, m, ArH), 7.78−7.62 (1.5 H, m, ArH), 7.46 (0.5 H, d, $J =$ 8.1 Hz, ArH), 7.25−7.10 (2 H, m, ArH and Voc), 6.50 (0.5 H, m, 3-H), 6.42 (0.5 H, m, 3-H), 5.44 (0.5 H, br d, $J =$ 9.2 Hz, 1-H), 5.29 (0.5 H, br d, $J =$ 9.0 Hz, 1-H), 4.78 (0.5 H, d d, $J =$ 14.0, 1.6 Hz, Voc), 4.62−4.52 (1 H, m, 6-H), 4.43 (0.5 H, d d, $J =$ 6.3, 1.5 Hz, Voc), 4.28 (0.5 H, d d, $J =$ 14.0, 1.3 Hz, Voc), 4.24 (0.5 H, d d, $J =$ 6.3, 1.5 Hz, Voc), 2.60−1.65 (8 H, m). MS (CI): m/z 271 (M$^+$ + H, 49), 227 (100). HRMS: calcd for C$_{16}$H$_{19}$N$_2$O$_2$ (MH$^+$), 271.1446; found, 271.1442.

2-(3-Pyridinyl)-9-vinyloxycarbonyl-9-azabicyclo[4.2.1]-non-2-ene (11a). Colorless oil, isolated in 70% yield. IR (film) ν (cm^{-1}): 1714, 1422. ^1H NMR (400 MHz, CDCl$_3$): 8.63 (0.5 H, d, $J =$ 2 Hz, 2′-H), 8.61 (0.5 H, d, $J =$ 2 Hz, 2′-H), 8.49 (1 H, d d d, $J =$ 7.8, 4.9, 1.5 Hz, 5′-H), 8.13 (0.5 H, d d d, $J =$ 7.8, 2.0, 2.0 Hz, 4′-H), 7.75 (0.5 H, d d d, $J =$ 7.8, 2.0, 2.0 Hz, 4′-H), 7.32−7.19 (2 H, m, 6′-H and Voc), 5.91 (1 H, m), 4.90 (1 H, m), 4.80 (0.5 H, d d, $J =$ 14, 1.6 Hz, Voc), 4.58 (1.5 H, m, Voc) 4.47 (0.5 H, d d, $J =$ 6.4, 1.7 Hz, voc), 4.40 (0.5 H, d d, $J =$ 6.4, 1.7 Hz, voc), 2.50−168 (8 H, m). ^{13}C NMR (75.5 MHz, CDCl$_3$): 150.7/150.4 (C), 147.9/147.5 (CH), 147.4/147.1 (CH), 146.0/ 145.4 (C) 142.3/142.1 (CH), 138.1/137.8 (C), 135.0/133.7 (CH), 130.0/129.8 (CH), 123.35/123.1 (CH), 95.3/95.2 (CH$_2$), 59.1/58.8 (CH), 56.6 (CH) 32.0/31.8 (CH$_2$), 31.2/30.7 (CH$_2$) 29.0/28.3

(CH$_2$), 24.1/24.0 (CH$_2$). MS (CI): m/z 271 (M$^+$ + 173), 227 (100). HRMS: calcd for C$_{16}$H$_{19}$N$_2$O$_2$ (MH$^+$), 271.1446; found, 271.1442.

2-(4-Pyridinyl)-9-vinyloxycarbonyl-9-azabicyclo[4.2.1]-non-2-ene (11c). Freshly cut lithium (106 mg, 15.32 mmol) and naphthalene (1.99 g, 15.57 mmol) in dry THF (15 mL) under a nitrogen atmosphere were stirred at room temperature for 2 h. After this time, 0.95 mL of this solution was removed and transferred to a clean, dry flask. Anhydrous zinc chloride (0.5 M in THF, 0.97 mL, 0.485 mmol) was added dropwise over 10 min. 2-(3-Bromo-4-pyridinyl)-9-vinyloxycarbonyl-9-azabicyclo-[4.2.1]non-2-ene (Spencer et al., 2001.) (85 mg, 0.243 mmol) in dry THF (4 mL) was added, and the suspension was heated to reflux for 1 h. The mixture was allowed to cool and quenched with water (10 mL). The organic phase was separated, and the aqueous phase was extracted with dichloromethane (2 × 10 mL) followed by ethyl acetate (3 × 10 mL). The combined organic residues were dried (Na$_2$SO$_4$), and the solvent was removed in vacuo. The residue was purified by flash chromatography (1:2 ethyl acetate/hexane) to give the title compound **11c** (55 mg, 83%) as a colorless oil. IR (CHCl$_3$) ν (cm^{-1}): 1711, 1425. ^{1}H NMR (270 MHz, CDCl$_3$): 8.55 (2 H, m, ArH), 7.55 (1 H, m, ArH), 7.31 (1 H, m, ArH), 7.24 (0.5 H, d d, J = 14.2, 6.3 Hz, Voc), 7.18 (0.5 H, d d, J = 14.2, 6.3 Hz, Voc), 6.10 (1 H, m, 3-H), 4.96 (1 H, m, 1-H), 4.80 (0.5 H, d d, J = 13.8, 1.6 Hz, Voc), 4.60 (1 H, m, 6-H), 4.50 (0.5 H, d d, J = 13.8, 1.6 Hz, Voc), 4.46 (0.5 H, d d, J = 6.3, 1.6 Hz, Voc), 4.37 (0.5 H, d d, J = 6.3, 1.6 Hz, Voc), 2.56–1.64 (8 H, m, C*H*$_2$). MS (CI): m/z 271 (MH$^+$, 66%), 227 (100), 199 (30). HRMS: calcd for C$_{16}$H$_{19}$N$_2$O$_2$ (MH$^+$), 271.1446; found, 271.1458.

2-(3-Pyridazinyl)-9-vinyloxycarbony-9-azabicyclo[4.2.1]-non-2-ene (11d). Colorless oil, isolated in 87% yield. IR (CHCl$_3$) ν (cm^{-1}): 1715, 1430. ^{1}H NMR (270 MHz, CDCl$_3$): 9.05 (1 H, br t, J = 9 Hz, 6′-H), 7.88 (0.5 H, d d, J = 9, 1 Hz, 4′-H), 7.68–7.40 (1.5 H, m), 7.22 (1 H, m), 6.40 (1 H, m, 3-H), 5.67 (0.5 H, br d, J = 9 Hz, 1-H), 5.31 (0.5 H, br d J = 9 Hz, 1-H), 4.80 (0.5 H, d d, J = 13.8, 1.6 Hz, Voc), 4.60 (1 H, m, 6-H), 4.50 (0.5 H, d d, J = 13.8, 1.6 Hz, Voc), 4.46 (0.5 H, d d, J = 6.3, 1.6 Hz, Voc), 4.37 (0.5 H, d d, J = 6.3, 1.6 Hz, Voc), 2.58–2.52 (3 H, m), 2.30–2.01 (5 H, m). MS (60 eV): m/z 271 (M$^+$, 100), 228 (95). HRMS: calcd for C$_{15}$H$_{17}$N$_3$O$_2$, 271.1321; found, 271.1320.

2-(5-Pyrimidinyl)-9-vinyloxycarbonyl-9-azabicyclo[4.2.1]-non-2-ene (11e). Colorless solid, isolated in 77% yield; mp 85–86 °C (toluene). IR (CHCl$_3$) ν (cm^{-1}): 1705, 1648, 1424. ^{1}H NMR (CDCl$_3$, 270 MHz): 9.12 (1 H, s, ArH), 8.95 (1 H, s, ArH), 8.80 (1 H, s, ArH), 7.22 (1 H, m, Voc), 5.97 (1 H, m, 3-H), 4.89 (1 H, m, 1-H), 4.82 (0.5 H, d d, J = 13.8, 1.6 Hz, Voc), 4.61 (1.5 H, m, Voc and 6-H), 4.48 (0.5 H, d d, J = 6.6, 1.6 Hz, Voc), 4.43 (0.5 H, d d, J = 6.8, 1.6 Hz, Voc), 2.58–1.80 (8 H, m). MS (CI): m/z 272 (MH$^+$, 65%), 228 (100), 185 (35). HRMS: calcd for C$_{15}$H$_{18}$N$_3$O$_2$ (MH$^+$), 272.1399; found, 272.1391.

2-(2-Pyrazinyl)-9-vinyloxycarbonyl-9-azabicyclo[4.2.1]-non-2-ene (11f). Colorless oil, isolated in 80% yield. IR (CHCl$_3$) ν (cm^{-1}): 1707, 1648. ^{1}H NMR (270 MHz, CDCl$_3$): 8.85 (0.5 H, d, J = 1 Hz, 3′-H), 8.77 (0.5 H, d, J = 1 Hz, 3′-H), 8.53–8.39 (2 H, m, 5′-H and 6′-H), 7.20 (1 H, m, Voc), 6.51 (1 H, m, 3-H), 5.48 (1H, m, 1-H), 4.78 (0.5 H, d d, J = 14, 1.5 Hz, Voc), 4.60 (1 H, m, 6-H), 4.48 (0.5 H, d d, J = 14, 1.5 Hz, Voc), 4.29 (1 H, m, Voc), 2.75–1.80 (8 H, m). MS (60 eV): m/z 271 (M$^+$, 10), 228 (100). HRMS: calcd for C$_{15}$H$_{17}$N$_3$O$_2$, 271.1321; found, 271.1331.

General Procedure 2. Acid-mediated cleavage of N-vinyloxycarbonyl group was performed to give compounds **4–9**.

2-(2-Pyridinyl)-9-azabicyclo[4.2.1]non-2-ene Hydrochloride Salt (5). To a solution of 2-(2-pyridinyl)-9-vinyloxycarbonyl-9-azabicyclo[4.2.1]non-2-ene (42 mg, 0.156 mmol) in dioxane (6 mL) were added water (1 mL) and concentrated hydrochloric acid (0.2 mL). The mixture was heated at reflux for 22 h and then allowed to cool. The majority of the dioxane was evaporated in vacuo, and the residue was diluted with water (5 mL), cooled to 0 °C, and made basic by the dropwise addition of 5 M NaOH solution. The basic solution was extracted with dichloromethane (5 × 10 mL), and the combined organic phases were evaporated in vacuo to give the title

compound **5** in quantitative yield as a colorless glass. ^{1}H NMR (300 MHz, CD$_3$OD): 8.76 (1 H, m, ArH), 8.59 (1 H, t, J = 8.0 Hz, ArH), 8.17 (1 H, d, J = 8.2 Hz, ArH), 7.97 (1 H, m, ArH), 6.95 (1 H, m, 3-H), 4.90 (1 H, d, J = 8.5 Hz, 1-H), 4.38 (1 H, m, 6-H), 2.88–2.62 (3 H, m), 2.44–1.94 (5 H, m). ^{13}C NMR (75.5 MHz, CD$_3$OD): 153.7 (C), 148.2 (CH), 147.7 (CH), 142.5 (CH), 136.8 (C), 127.0 (2 x CH), 61.2 (CH), 59.1 (CH), 32.2 (CH$_2$), 28.7 (CH$_2$), 25.2 (CH$_2$), 24.8 (CH$_2$). MS (70 eV): m/z 200 (M$^+$, 69%), 171 (66), 105 (100). HRMS: calcd for C$_{13}$H$_{16}$N$_2$, 200.1313; found, 200.1310.

2-(3-Pyridinyl)-9-azabicyclo[4.2.1]non-2-ene Hydrochloride Salt (4). Colorless glass. ^{1}H NMR (400 MHz, CDCl$_3$): 10.20 (2 H, br, NH), 9.28 (1 H, br, ArH), 8.62 (1 H, br, ArH), 8.46 (1 H, br, ArH), 7.90 (1 H, br, ArH), 6.41 (1 H, m, H-3), 5.00 (1 H, m), 4.46 (1 H, m), 2.79–1.50 (8 H, m). ^{13}C NMR (75.5 MHz, CDCl$_3$): 147.7 (CH), 147.5 (CH), 143.8 (C), 139.8 (C), 133.3 (CH), 130.5 (CH), 123.0 (CH), 65.5 (CH), 62.1 (CH), 32.2 (CH$_2$), 28.4 (CH$_2$), 24.8 (CH$_2$), 24.6 (CH$_2$). MS (CI): m/z 201 (M$^+$, 100). HRMS: calcd for C$_{13}$H$_{17}$N$_2$ (MH$^+$), 201.1392; found, 201.1384.

2-(4-Pyridinyl)-9-azabicyclo[4.2.1]non-2-ene Hydrochloride Salt (6). Colorless glass. ^{1}H NMR (270 MHz, CD$_3$-NO$_2$): 10.47 (1 H, broad s, NH), 9.79 (1 H, broad s, NH), 8.71 (2 H, br s, ArH), 8.04 (2 H, br s, ArH), 6.86 (1 H, m, 3-H), 4.84 (1 H, m, 1-H), 4.42 (1 H, m, 6-H), 2.86–1.91 (8 H, m, CH$_2$). ^{13}C NMR (75.5 MHz, CD$_3$NO$_2$): 150.3 (CH), 145.0 (C), 136.4 (C), 126.8 (CH), 123.8 (CH), 60.9 (CH), 59.2 (CH), 32.1 (CH$_2$), 28.4 (CH$_2$), 25.0 (CH$_2$), 24.8 (CH$_2$). MS (CI): m/z 201 (MH$^+$, 100%). HRMS: calcd for C$_{13}$H$_{17}$N$_2$, 201.1392; found, 201.1392.

2-(3-Pyridazinyl)-9-azabicyclo[4.2.1]non-2-ene Hydrochloride Salt (7). ^{1}H NMR (300 MHz, CD$_3$OD): 9.07 (1H, d d, J = 5, 1.5 Hz, 6′-H), 7.95 (1 H, d d, J = 8, 1.5 Hz, 4′-H), 7.64 (1H, d d, J = 8, 5 Hz, 5′-H), 6.88 (1 H, m, 3-H), 5.53 (1 H, br d, J 9.5 Hz, 1-H), 4.32 (1 H, m, 6-H), 2.70–2.05 (8 H, m). ^{13}C NMR (75.5 MHz, CD$_3$OD): 160.0, 150.1, 140.5, 138.6, 127.9, 124.5, 63.8 (CH), 58.0 (CH), 30.4 (CH$_2$), 28.1 (CH$_2$), 27.2 (CH$_2$), 23.2 (CH$_2$). MS (60 eV): m/z 201 (M$^+$, 100), 172 (90). HRMS: calcd for C$_{12}$H$_{15}$N$_3$, 201.1266; found, 201.1266.

2-(5-Pyrimidinyl)-9-azabicyclo[4.2.1]non-2-ene Hydrochloride Salt (8). Colorless glass. δ_H (270 MHz, CD$_3$NO$_2$): 9.96 (1 H, broad s, NH), 9.70 (1 H, broad s, NH), 9.57 (2 H, s, ArH), 9.43 (1 H, s, ArH), 6.67 (1 H, m, 3-H), 4.86 (1 H, m, 1-H), 4.46 (1 H, m, 6-H), 2.86–1.92 (8 H, m). ^{13}C NMR (75.5 MHz, CD$_3$NO$_2$): 157.0 (CH), 154.7 (CH), 144.1 (C), 136.0 (C), 131.4 (CH), 60.1 (CH), 59.0 (CH), 30.7 (CH$_2$), 28.0 (CH$_2$), 27.1 (CH$_2$), 23.5 (CH$_2$). MS (CI): m/z 202 (MH$^+$, 100%), 185 (10), 173 (9), 159 (9), 133 (8), 82 (9). HRMS: calcd for C$_{12}$H$_{16}$N$_3$ (MH$^+$), 202.1344; found, 202.1346.

2-(2-Pyrazinyl)-9-azabicyclo[4.2.1]non-2-ene Hydrochloride Salt (9). Colorless glass. ^{1}H NMR (270 MHz, CD$_3$-OD): 9.14 (1 H, d, J = 1.6 Hz, 3′-H), 9.09 (1 H, d d, J = 3, 1.6 Hz, 5′-H), 8.68 (1 H, d, J = 3 Hz, 6′-H), 7.14 (1 H, m, 3-H), 5.37 (1 H, br d, J = 9.6 Hz, 1-H), 4.36 (1 H, m, 6-H), 2.75–2.02 (8 H, m). ^{13}C NMR (75.5 MHz, CD$_3$OD): 155.0 (C), 147.0 (C), 143.8 (CH), 141.9 (CH), 132.9 (CH), 130.0 (CH), 60.8 (CH), 59.0 (CH), 31.6, 29.0, 28.4, 24.7. MS (60 eV): m/z 201 (M$^+$, 100). HRMS: calcd for C$_{12}$H$_{15}$N$_3$, 201.1266; found, 201.1261.

Biology. Cell Culture. The mouse fibroblast Lα3β4 cell line stably transfected with the rat α3 and β4 subunit cDNAs were maintained as previously described.[27] Expression of nAChRs was induced by 1 μM dexamethasone.

Membrane Preparation. Rat P2 brain membranes were prepared as described previously.[9] Membranes from Lα3β4 cells were prepared as follows: cells were briefly washed once with phosphate-buffered saline (PBS, 150 mM NaCl, 2 mM KH$_2$PO$_4$, 8 mM K$_2$HPO$_4$, pH 7.4) and scraped into ice-cold homogenization buffer (PBS, 10 mM EDTA, 10 mM EGTA, 1 mM PMSF, pH 7.4). Cells were pelleted by centrifugation (500 g, 3 min) and sonicated. The resulting homogenate was centrifuged (100 000 g, 30 min), and the membrane pellet was resuspended in ice-cold homogenization buffer by use of a hand held homogenizer. The membranes were stored in aliquots at −20 °C.

Radioligand Competition Binding Assays. (±)-[³H]-Epibatidine Binding. Lα3β4 cell membranes (10 μg of protein) were diluted into Krebs−Ringer Tris HEPES buffer (118 mM NaCl, 4.8 mM KCl, 2.5 mM CaCl$_2$, 20 mM HEPES, 20 mM Tris, 0.1 mM PMSF, 0.01% NaN$_3$, pH 7.4) containing 1 nM (±)-[³H]epibatidine and competing drugs to a total volume of 1 mL. Nonspecific binding was determined in the presence of 1 mM (−)-nicotine. Samples were incubated for 2 h at 37 °C before filtration through Gelman GFA/E filter paper (presoaked overnight in 0.3% polyethyleneimine in PBS) using a Brandel Cell Harvester. Filters were added to Optiphase Safe scintillation cocktail, and samples were counted for 5 min each in a Packard Tricarb scintillation counter.

(−)-[³H]Nicotine Binding and [³H]MLA Binding. Competition binding assays were performed as previously described.[9,25] In brief, rat brain P2 brain membranes (250 μg protein) were incubated with serial dilutions of competing drugs and 2 nM [³H]MLA for 2.5 h at room temperature or 10 nM [³H]nicotine for 30 min at room temperature plus 1 h at 4 °C, respectively. Bound and free radioligand was separated by filtration as described above. Nonspecific binding was determined in the presence of 1 mM (−)-nicotine.

Radioligand Binding Data Analysis. IC$_{50}$ values were calculated by fitting data points to the Hill equation, using the nonlinear least squares curve fitting facility of Sigma Plot V2.0 for Windows. K_i values were derived from IC$_{50}$ values according to the method of Cheng and Prusoff,[38] assuming K_d values of 5.6 and 1.86 nM for (−)-[³H]nicotine and [³H]MLA binding to rat brain membranes and 0.27 nM for (±)-[³H]-epibatidine binding to Lα3β4 cell membranes, respectively.

Calcium Fluorimetry. Lα3β4 cells were seeded into 96 well plates, and nAChR expression was induced for 7−10 days with 1 μM dexamethasone. On the day of assay, culture medium was removed, cells were washed twice with Tyrode's Salt Solution (TSS, 137 mM NaCl, 2.7 mM KCl, 1 mM MgCl$_2$, 1.8 mM CaCl$_2$, 0.2 mM NaH$_2$PO$_4$, 12 mM NaHCO$_3$, 5.5 mM glucose, pH 7.4) and loaded with 5 μM fluo-3 in 0.02% Pluronic acid/TSS for 1 h at room temperature in the dark. Unloaded fluo-3 was removed by washing cells twice with TSS, and the cells were incubated in TSS for a further 30 min at room temperature in the dark. Plates were transferred to a Fluoroskan Ascent (Labsystems, Helsinki, Finland), and TSS was replaced by 80 μL/well High Calcium Buffer (HCB, 75 mM CaCl$_2$, 35 mM sucrose, 25 mM HEPES, pH 7.4) containing agonist; fluorescence was monitored for 16 s. The peak fluorescent response was calibrated by determination of maximal and minimal fluorescence in the presence of 2% Triton X-100 and 40 mM MnCl$_2$, respectively. Changes in intracellular calcium were calculated as a percentage of the difference between the minimal and the maximal fluorescence and expressed as a percentage of the response given by a maximally stimulating concentration of (−)-nicotine (100 μM). EC$_{50}$ values were calculated by fitting data points to the Hill equation, using the nonlinear least squares curve fitting facility of Sigma Plot V2.0 for Windows.

Molecular Modeling. Ligands **4**−**6** were subjected to Monte Carlo conformational searching in Maestro (version 3.0.019) using Macromodel MMFF force field with a solvation model for water. The search was continued until all of the conformations had been found a minimum of 10 times. The lowest energy conformer was then subjected to dihedral driving around torsion C(1)−C(2)−C(3′)−C(2′) (see structure **1**) in 5 degree increments, and a graph was plotted against energy relative to the global minimum. The structures at the points defined in Figure 4a,b were constrained and minimized with dummy H-atoms from N(9) (anti to the four carbon bridge) and the pyridine nitrogen positioned to 2.9 Å (site points a and b, respectively). The N−N distances, as well as the (a−b) distance and the bac angle (Δbac), were measured at each point on the conformational profile and are summarized in Table 3.

Note Added in Proof. Following the submission of this paper, Steitz and co-workers[39] have reported independently on the synthesis and biological evaluation of enantiomerically pure **4** and diazine variants **7**−**9**, and the synthetic strategy used by these authors was adapted from that previously reported[19] for UB-165. Steitz and co-workers also describe computational results associated with the atomic electrostatic potential charges of the nitrogen atoms associated with the pyridyl and diazine ligands and apply these data to correlate the binding affinity and the hydrogen bond acceptor capacity of the heteroaryl moiety.

References

(1) Role, L. W.; Berg, D. K. Nicotinic receptors in the development and modulation of CNS synapses. *Neuron* **1996**, *16*, 1077−1085.

(2) Lukas, R. J.; Changeux, J.-P.; le Novère, N.; Albuquerque, E. X.; Balfour, D. J. K.; Berg, D. K.; Bertrand, D.; Chiappinelli, V. A.; Clarke, P. B. S.; Collins, A. C.; Dani, J. A.; Grady, S. A.; Kellar, K. J.; Lindstrom, J. M.; Marks, M. J.; Quik, M.; Taylor, P. W.; Wonnacott, S. International Union of Pharmacology. XX. Current status of the nomenclature for nicotinic acetylcholine receptors and their subunits. *Pharmacol. Rev.* **1999**, *51*, 397−401.

(3) Elgoyhen, A. B.; Vetter, D. E.; Katz, E.; Rothlin, C. V.; Heinemann, S. F.; Boulter, J. α 10: A determinant of nicotinic cholinergic receptor function in mammalian vestibular and cochlear mechanosensory hair cells. *Proc. Natl. Acad. Sci. U.S.A.* **2001**, *98*, 3501−3506.

(4) Seguela, P.; Wadiche, J.; Dineley-Miller, K.; Dani, J. A.; Patrick, J. W. Molecular cloning, functional properties, and distribution of rat brain alpha 7: a nicotinic cation channel highly permeable to calcium. *J. Neurosci.* **1993**, *13*, 596−604.

(5) Zoli, M.; Lena, C.; Picciotto, M. R.; Changeux, J.-P. Identification of four classes of brain nicotinic receptors using beta2 mutant mice. *J. Neurosci.* **1998**, *18*, 4461−4472.

(6) Cordero-Erausquin, M.; Marubio, L. M.; Klink, R.; Changeux, J.-P. Nicotinic receptor function: new perspectives from knockout mice. *Trends Pharmacol. Sci.* **2000**, *21*, 211−217.

(7) Chen, D.; Patrick, J. W. The alpha-bungarotoxin-binding nicotinic acetylcholine receptor from rat brain contains only the alpha7 subunit. *J. Biol. Chem.* **1997**, *272*, 24024−24029.

(8) Drisdel, R. C.; Green, W. N. Neuronal alpha-bungarotoxin receptors are alpha7 subunit homomers. *J. Neurosci.* **2000**, *20*, 133−139.

(9) Davies, A. R. L.; Hardick, D. J.; Blagborough, I. S.; Potter, B. V. L.; Wolstenholme, A. J.; Wonnacott, S. Characterisation of the binding of [³H]methylycaconitine: a new radioligand for labeling α7-type neuronal nicotinic acetylcholine receptors. *Neuropharmacology* **1999**, *38*, 679−690.

(10) Sivilotti, L. G.; McNeil, D. K.; Lewis, T. M.; Nassar, M. A.; Schoepfer, R.; Colquhoun, D. Recombinant nicotinic receptors, expressed in Xenopus oocytes, do not resemble native rat sympathetic ganglion receptors in single-channel behaviour. *J. Physiol.* **1997**, *500*, 123−138.

(11) Wang, F.; Nelson, M. E.; Kuryatov, A.; Olale, F.; Cooper, J.; Keyser, K.; Lindstrom, J. Chronic nicotine treatment upregulates human alpha3 beta2 but not alpha3 beta4 acetylcholine receptors stably transfected in human embryonic kidney cells. *J. Biol. Chem.* **1998**, *273*, 28721−28732.

(12) Jones, S.; Sudweeks, S.; Yakel, J. L. Nicotinic receptors in the brain: correlating physiology with function. *Trends Neurosci.* **1999**, *22*, 555−561.

(13) Holladay, M. W.; Dart, M. J.; Lynch, J. K. Neuronal nicotinic acetylcholine receptors as targets for drug discovery. *J. Med. Chem.* **1997**, *40*, 4169−4194.

(14) Beers, W. H.; Reich, E. Structure and activity of acetylcholine. *Nature* **1970**, *228*, 917−922.

(15) Sheridan, R. P.; Nilakantan, R.; Dixon, J. S.; Venkataraghavan, R. The ensemble approach to distance geometry: application to the nicotinic pharmacophore. *J. Med. Chem.* **1986**, *29*, 899−906.

(16) Tønder, J. E.; Olesen, P. H. Agonists at the α4β2 nicotinic acetylcholine receptors: Structure−activity relationships and molecular modelling. *Curr. Med. Chem.* **2001**, *8*, 651−674.

(17) Brejc, K.; van Dijk, W. J.; Klaassen, R. V.; Schuurmans, M.; van Der Oost, J.; Smit, A. B.; Sixma, T. K. Crystal structure of an ACh-binding protein reveals the ligand-binding domain of nicotinic receptors. *Nature* **2001**, *411*, 269−276.

(18) Tønder, T. E.; Olesen, P. H.; Hansen, J. B.; Begtrup, M.; Pettersson, I. An improved nicotinic pharmacophore and a stereoselective CoMFA-model for nicotinic agonists acting at the central nicotinic acetylcholine receptors labeled by [³H]-*N*-methylcarbamylcholine. *J. Comput.-Aided Mol. Des.* **2001**, *15*, 247−258.

(19) Wright, E.; Gallagher, T.; Sharples, C. G. V.; Wonnacott, S. Synthesis of UB-165: a novel nicotinic ligand and anatoxin-a/epibatidine hybrid. *Bioorg. Med. Chem. Lett.* **1997**, *7*, 2867−2870.

(20) Swanson, K. L.; Allen, C. N.; Aronstam, R. S.; Rapoport, H.; Albuquerque, E. X. Molecular mechanisms of the potent and stereospecific nicotinic agonist (+)-anatoxin-a. *Mol. Pharmacol.* **1986**, *29*, 250−257.

(21) Macallan, D. R.; Lunt, G. G.; Wonnacott, S.; Swanson, K. L.; Rapoport, H.; Albuquerque, E. X. Methyllycaconitine and (+)-anatoxin-a differentiate between nicotinic receptors in vertebrate and invertebrate nervous systems. *FEBS Lett.* **1988**, *226*, 357−363.

(22) Badio, B.; Daly, J. W. Epibatidine, a potent analgetic and nicotinic agonist. *Mol. Pharmacol.* **1994**, *45*, 563−569.

(23) Dukat, M.; Damaj, M. I.; Glassco, W.; Dumas, D.; May, E. L.; Martin, B. R.; Glennon, R. A. Epibatidine: A Very High Affinity Nicotine-receptor Ligand. *Med. Chem. Res.* **1993**, *4*, 131−139.

(24) Badio, B.; Garraffo, H. M.; Spande, T. F.; Daly, J. W. Epibatidine: Discovery and definition as a potent analgesic and nicotinic agonist. *Med. Chem. Res.* **1994**, *4*, 440−448.

(25) Sharples, C. G. V.; Kaiser, S.; Soliakov, L.; Marks, M. J.; Collins, A. C.; Washburn, M.; Wright, E.; Spencer, J. A.; Gallagher, T.; Whiteaker, P.; Wonnacott, S. UB-165: A novel nicotinic agonist with subtype selectivity implicates the α4β2* subtype in the modulation of dopamine release from rat striatal synaptosomes. *J. Neurosci.* **2000**, *20*, 2783−2791.

(26) Spencer, J. A.; Karig, G.; Gallagher, T. Directed deprotonation-transmetalation as a route to substituted pyridines. *Org. Lett.* **2001**, *3*, 835−838.

(27) Lewis, T. M.; Harkness, P. C.; Sivilotti, L. G.; Colquhoun, D.; Millar, N. S. The ion channel properties of a rat recombinant neuronal nicotinic receptor are dependent on the host cell type. *J. Physiol.* **1997**, *505*, 299−306.

(28) Dukat, M.; Fiedler, W.; Dumas, D.; Damaj, I.; Martin, B. R.; Rosecrans, J. A.; James, J. R.; Glennon, R. A. Pyrrolidine-modified and 6-substituted analogues of nicotine: a structure-affinity investigation. *Eur. J. Med. Chem.* **1996**, *31*, 875−888.

(29) Dart, M. J.; Wasicak, J. T.; Ryther, K. B.; Schrimpf, M. R.; Kim, K. H.; Anderson, D. J.; Sullivan, J. P.; Meyer, M. D. Structural aspects of high affinity ligands for the α4β2 neuronal nicotinic receptor. *Pharm. Acta Helv.* **2000**, *74*, 115−123.

(30) Nobeli, I.; Price, S. L.; Lommerse, J. P. M.; Taylor, R. Hydrogen bonding properties of oxygen and nitrogen acceptors in aromatic heterocycles. *J. Comput. Chem.* **1997**, *18*, 2060−2074.

(31) Abraham, M. H.; Duce, P. P.; Prior, D. V.; Barratt, D. G.; Morris, J. J.; Taylor, P. J. Hydrogen bonding 9. Solute proton donor and proton acceptor scales for use in drug design. *J. Chem. Soc., Perkin Trans. 2* **1989**, 1355−1375.

(32) Seerden, J.-P. G.; Tulp, M. T. M.; Scheeren, H. W.; Kruse, C. G. Synthesis and structure−activity data of some new epibatidine analogues. *Biol. Med. Chem.* **1998**, *6*, 2103−2110.

(33) Spang, J. E.; Bertrand, S.; Westera, G.; Patt, J. T.; August Schubiger, P.; Bertrand D. Chemical modification of epibatidine causes a switch from agonist to antagonist and modifies its selectivity for neuronal nicotinic acetylcholine receptors. *Chem. Biol.* **2000**, *7*, 545−555.

(34) Marks, M. J.; Robinson, S. F.; Collins, A. C. Nicotinic agonists differ in activation and desensitization of 86Rb+ efflux from mouse thalamic synaptosomes. *J. Pharmacol. Exp. Ther.* **1996**, *277*, 1383−1396.

(35) Glennon, R. A.; Herndon, J. A.; Dukat, M. Epibatidine-aided studies toward definition of a nicotinic receptor pharmacophore. *Med. Chem. Res.* **1994**, *6*, 465−486.

(36) Tønder, T. E.; Hansen, J. B.; Begtrup, M.; Pettersson, I.; Rimvall, K.; Christensen, B.; Ehrbar, U.; Olesen, P. H. Improving the nicotinic pharmacophore with a series of (Isoxazole)methylene-1-azacyclic compounds: synthesis, structure−activity relationship and molecular modelling. *J. Med. Chem.* **1999**, *42*, 4970−4980.

(37) Manallack, D.; Gallagher, T.; Livingstone, D. Quantitative Structure−Activity Relationships of Nicotinic Agonists. *Principles in QSAR and Drug Design*; Devillers, J., Ed.; Academic Press: New York, 1996; Vol. 2, pp 177−208.

(38) Cheng, Y.-C.; Prusoff, W. H. Relationship between the inhibition constant (K_i) and the concentration of the inhibitor which causes 50% inhibition (IC_{50}) an enzymatic reaction. *Biochem. Pharmacol.* **1973**, *22*, 3089−3108.

(39) Gohlke, H.; Gündisch, D.; Schwarz, S.; Seitz, G.; Tilotta, M. C.; Wegge, T. Synthesis and Nicotinic Binding Studies on Enantiopure Diazine Analogues of the Novel (2-Chloro-5-pyridyl)-9-azabicyclo[4.2.1]non-2-ene UB-165. *J. Med. Chem.* **2002**, *45*, 1064−1072.